LIQUID CRYSTALS, 2000, VOL. 27, NO. 2, 269–276

Pre-resonance Raman studies of some mesogens—TB4A, TB7A and TB10A

S. K. DASH*
Parts and Materials Division (SRG), ISRO Satellite Centre, Bangalore—560 017, India

RANJAN K. SINGH
Department of Physics, Jay Prakash University, Chapra—841 301, India

P. R. ALAPATI
Department of Physics, North Eastern Regional Institute of Science and Technology, Itanagar—791 109, India

and A. L. VERMA
Department of Physics, North Eastern Hill University, Shillong—793 022, India

(*Received 11 May 1999; in final form 8 September 1999; accepted 15 September 1999*)

Pre-resonance Raman spectra of certain liquid crystalline compounds, TB4A, TB7A and TB10A, are reported. The anomaly observed in the pre-resonance Raman spectra in the three compounds was initially explained by the Albrecht–Hutley Model, but its failure leads us to explain the anomalous intensity enhancement mechanism by invoking an interference effect between a weak dipole-forbidden excited state and a nearby strong electronic level via vibrational modes. The presence of a 2^1A_g dipole-forbidden excited state in TB4A and TB10A is deduced after an elaborate discussion of their centro-symmetric structure. The structural difference of TB7A in comparison with TB4A and TB10A is also discussed by taking their X-ray data into consideration.

1. Introduction

Vibrational spectroscopy has been a matter of great interest in both experimental and theoretical research for a long time. Especially, in recent years, Raman spectroscopy has been a very useful tool in the investigation of the vibrational dynamics of liquid crystalline compounds. The spectra–structure correlation, as well as the connection between structural phase changes and the corresponding changes in the Raman spectra, are of particular interest. These aspects have been potentially exploited in order to obtain information about different molecular configurations [1–8] such as molecular orientation [9], inter/intra-molecular interactions [10], etc. Enhancement of Raman intensities in the resonance and pre-resonance region [11–16] has also attracted considerable attention. The resonance Raman theory is primarily based on the Kramers–Heisenberg–Dirac relation and has been explained by many authors [11–14] in various ways. The Albrecht [12] theory which is initially used here for explaining the Raman excitation profile (REP), expresses the Raman cross-section directly in terms of molecular parameters. Rigorous Raman resonance occurs when the exciting radiation frequency falls within the observable vibrational structure, whereas the pre-resonance Raman effect is observed when the exciting radiation frequency falls within the high or low frequency wings, but not under the observable vibrational structure of the electronic absorption band involved in the Raman scattering process. The variation of Raman intensity in different vibrational modes as a function of incident laser photon energy, commonly known as the excitation profile, is important for obtaining information about, for example, the properties of a molecule in the electronic excited state, the vibrational mode and the atomic displacement between the ground and excited states [15].

When the energy of the exciting light approaches an electronic energy level, a monotonic increase of intensity of different Raman modes occurs in the pre-resonance region [11–16] due to vibronic coupling. Many models

*Author for correspondence; e-mail: sarat@isac.ernet.in

Liquid Crystals ISSN 0267-8292 print/ISSN 1366-5855 online © 2000 Taylor & Francis Ltd
http://www.tandf.co.uk/journals/tf/02678292.html

[11–14] have been proposed to explain the intensity enhancement theoretically in the pre-resonance region. However, the agreement of these models with experimental results is only approximate and sometimes they fail to account for the observed enhancement in many systems [17, 18]. It has been suggested that vibronic coupling between the electronically allowed and some forbidden transitions may lead to such inconsistency [17, 18], and sometimes such anomalies were explained by invoking the interference effect between electronic levels and weakly allowed or forbidden electronic levels via vibrational modes [19].

In the present study, the Raman excitation profiles (in the pre-resonance region) of some Raman bands for three thermotropic liquid crystalline compounds, TB4A, TB7A and TB10A are reported. These liquid crystalline compounds are basically Schiff's base compounds and differ in their long aliphatic chains. The staggered core [20, 21] consists of three benzene rings connected by Schiff's base linkages; the middle benzene ring is symmetrically substituted and the peripheral benzene rings are unsymmetrically substituted. The long saturated aliphatic chains attached to both ends of the core have a zig-zag structure. An overall structure for the three compounds is given below.

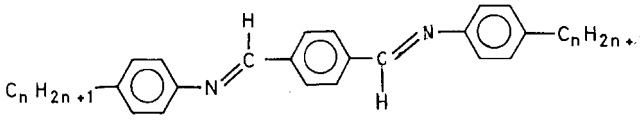

An attempt has been made here to explain the anomalous intensity enhancement in the pre-resonance Raman spectra of TB4A, TB7A and TB10A, an effect which is unaccountable in the Albrecht and Hutley model by invoking the interference effect between electronic levels and weakly allowed or forbidden electronic levels via vibrational modes.

2. Experimental

The liquid crystalline compounds TB4A, TB7A and TB10A were synthesized following a standard procedure [22, 23] and purified by repeated crystallization from an absolute ethanol–benzene mixture until the observed transition temperatures were constant. The Raman spectra in the 1100–1700 cm^{-1} region for TB4A, TB7A and TB10A dissolved in a non-interacting solvent ($CHCl_3$), were obtained on a spex Ramalog 1403 double monochromator equipped with an RCA-31034 photomultiplier tube and CCD detector using 514.5, 496.5, 488.0, 476.5, 457.5 nm lines from an Ar^+-ion laser and the 441.6 nm line from a He-Cd laser as excitation sources. A slit combination of 200-400-400-200 μm, a slit band pass of 2.5 cm^{-1}, a scanning increment of 1.0 cm^{-1} and an integration time of 1.0 s were found suitable in order to record the spectra with good signal to noise ratio. A DM-3000 series computer with Spectramax software was used to control the spectrometer and process the data. Electronic absorption spectra were recorded by a Cary 2390 UV-Vis spectrophotometer.

3. Discussion

First the assignment of all the observed bands in the 1100–1700 cm^{-1} region along with their depolarization ratios was made on the basis of earlier studies on similar compounds [24] and expected group frequencies [25] and is given in table 1. Representative Raman spectra for one of the samples (TB7A) as a function of exciting line wavelength are given in figure 1. As is evident from this figure, intensity enhancement is observed for almost all the ring modes as well as for modes associated with the Schiff's base linkages.

The electronic absorption spectra for TB4A, TB7A and TB10A are shown in figure 2. Strong absorption bands at ~363 and ~296 nm appear in the spectra of all these compounds. The strong band at ~363 nm is considered to arise from a major active electronic state in the TB4A, TB7A and TB10A systems. The other observed band at ~296 nm is located reasonably away from the excitation lines used and hence its contribution has been neglected for the intensity enhancement. It is to be noted here that the observed absorption bands in all the compounds are symmetrical and have nearly constant relative intensity ratios, thus reflecting a negligible effect of chain length. Again all the Raman bands chosen for this study are symmetrical with a depolarization

Table 1. Assignment and depolarization ratios of Raman bands considered for pre-resonance studies of TB4A, TB7A and TB10A. The band positions given in the table are approximately the same for the three systems.

Band position/cm^{-1}	Assignment	Depolarization ratio
1165	Aromatic C–H in plane bending mode (ν_{9a})	0.28
1195	Aromatic C–N stretching mode ($\nu_{\phi\text{-}N}$)	0.35
1563	Quadrant stretching of benzene ring (ν_{8a}')	0.34
1594	Quadrant stretching of benzene ring (ν_{8a})	0.30
1625	C=N stretching mode ($\nu_{C=N}$)	0.33

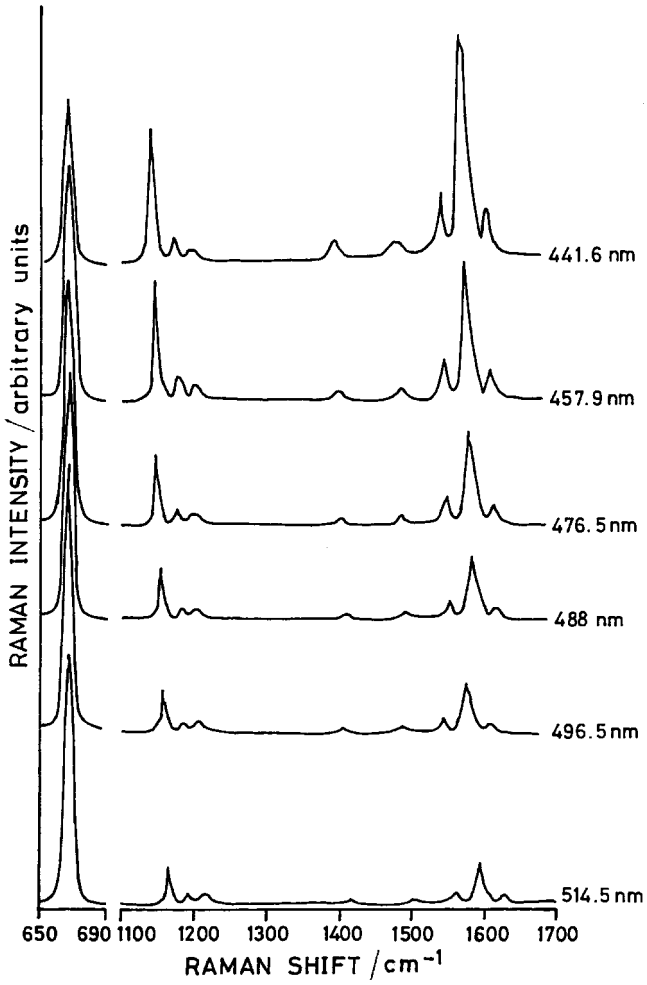

Figure 1. Raman spectra of TB7A in $CHCl_3$ with six different excitation lines.

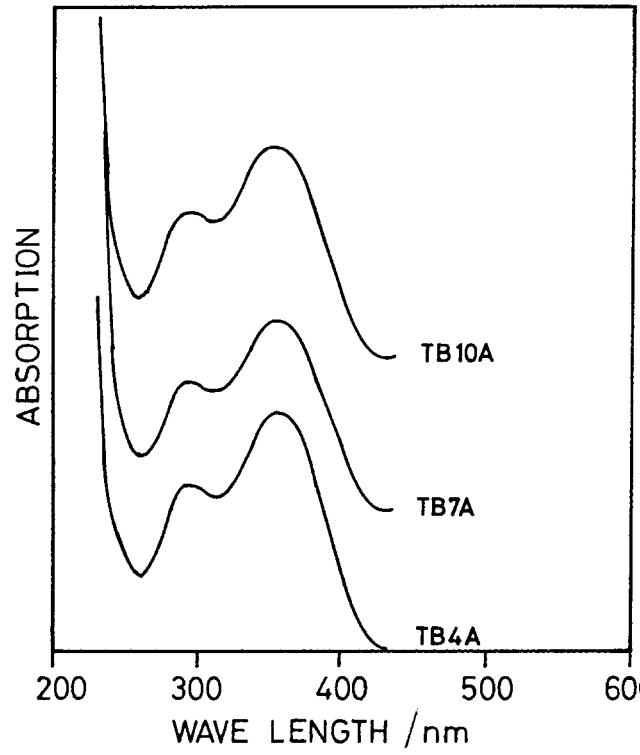

Figure 2. Electronic absorption spectra of the three compounds in $CHCl_3$.

ratio of 0.3 (see table 1). Therefore it is expected that the Albrecht and Hutley model may explain the intensity enhancement in the pre-resonance region.

When the frequency of the exciting radiation approaches an electronic state which serves as a major active state for the vibrational mode involved, the intensity enhancement is predicted to be governed by the frequency dependent dimensionless factor F_A given by Albrecht and Hutley [11] as

$$F_A = \frac{v^2 (v_e^2 + v_0^2)}{(v_e^2 - v_0^2)^2}. \quad (1)$$

However, if there is another electronic state, other than the major electronic state, the intensity enhancement is dependent on their vibronic coupling via vibrational modes and is predicted to be governed by the frequency dependent factor F_B given by Albrecht and Hutley [11] as

$$F_B = \frac{2v^2 (v_e v_s + v_0^2)}{(v_e^2 - v_0^2)(v_s^2 - v_0^2)} \quad (2)$$

where v_0, v, v_e and v_s refer to the frequency of the exciting radiation, scattered radiation, major active electronic state and virtual electronic state (other active higher electronic state), respectively. The approximation adopted in the 'A' term (Condon approximation) [15] is equivalent to assuming that the value of the electronic transition moment is independent of the vibrational transition accompanying the electronic transition and only a totally symmetric vibration gives rise to resonance enhancement via the Albrecht 'A' term [15]. Unlike the 'A' term, the 'B' term arises due to vibronic mixing of two excited electronic states via both totally symmetric and non-totally symmetric fundamental modes, provided that they are energetic enough for such coupling. The approximation adopted for the 'B' term is non-Condonian in nature [15]. In short, the 'A' term corresponds to intensity enhancement due to the active electronic state and the 'B' term refers to the vibronic coupling of the major active electronic state with other active higher electronic states (if any) having similar polarization. If the Raman intensity is uniquely governed by one of the terms given by equations (1) or (2), the

intensity $I_{m,n}$ may be written as [11]

$$I_{m.n} \propto F_A^2 \tag{3}$$

or

$$I_{m.n} \propto F_B^2. \tag{4}$$

In order to calculate the frequency dependent factors for TB4A, TB7A and TB10A, the v_e values have been taken as 8.174×10^{14} Hz ($\lambda = 367$ nm), 8.321×10^{14} Hz ($\lambda = 360$ nm), 8.253×10^{14} Hz ($\lambda = 363.5$ nm), respectively, corresponding to the strongest near-ultraviolet electronic absorption bands of TB4A, TB7A and TB10A (see figure 2). In addition, the TB4A, TB7A, and TB10A systems possess a second strong absorption band at an energy corresponding to ~ 296 nm. The frequency factor F_B is calculated by taking these absorption bands at ~ 296 nm for each respective system (see figure 2). In order to make an easy comparison of the theoretically predicted and experimentally observed intensity enhancement, dimensionless factors R_A, R_B and R_I are given as:

$$R_A = \frac{(F_A)^2_{\lambda 0}}{(F_A)^2_{4880}} \quad R_B = \frac{(F)^2_{\lambda 0}}{(F_B)^2_{4880}} \quad R_I = \frac{I_{\lambda 0}}{I_{4880}} \tag{5}$$

and have been calculated for every band at every excitation line under consideration. The v_1 mode of $CHCl_3$ at $\sim 667\,cm^{-1}$ has been used as an internal standard to calculate the experimentally observed intensity enhancement factor, R_I. Correction for the v^4 dependence of the intensity of the internal standard mode has been made separately. The relative intensities used for the calculations are peak intensities, since the line widths of various bands do not show appreciable change.

The values of R_A, R_B and R_I thus calculated, are given in tables 2 to 6 for the five most prominent bands, viz. 1625, 1594, 1563, 1193, and 1165 cm^{-1} for the three compounds. Other bands in the frequency range 1100–1700 cm^{-1} for all the compounds show similar trends in intensity enhancement. The observed Raman excitation profiles (REP) for the 1625 cm^{-1} band are shown in figures 3(*a*,*b*,*c*) for the three compounds TB4A, TB7A and TB10A, respectively. Similar band profiles are observed for other bands, but are not shown for the sake of brevity. We find that neither the R_A nor the R_B term accounts for the observed intensity enhancement (see figures 3(*a*,*b*,*c*) and tables 2 to 6). Interestingly, for TB4A and TB10A, the intensity enhancement profile

Table 2. Theoretically calculated and experimentally observed intensity enhancement for the 1625 cm^{-1} Raman band in terms of the R_A, R_B and R_I factors for TB4A, TB7A and TB10A.

	TB4A			TB7A			TB10A		
λ_o/Å	R_A	R_B	R_I	R_A	R_B	R_I	R_A	R_B	R_I
5145	0.67	0.76	0.36	0.68	0.76	0.59	0.68	0.76	0.58
4965	0.87	0.91	0.69	0.88	0.93	0.73	0.88	0.91	0.74
4880	1	1	1	1	1	1	1	1	1
4765	1.22	1.15	1.74	1.24	1.40	1.41	1.22	1.14	1.53
4579	1.78	1.47	3.20	1.72	1.45	2.55	1.74	1.45	3.85
4416	2.65	1.90	2.33	2.49	1.84	5.60	2.56	1.86	2.65

Table 3. Theoretically calculated and experimentally observed intensity enhancement for the 1594 cm^{-1} Raman band in terms of the R_A, R_B and R_I factors for TB4A, TB7A and TB10A.

	TB4A			TB7A			TB10A		
λ_o/Å	R_A	R_B	R_I	R_A	R_B	R_I	R_A	R_B	R_I
5145	0.67	0.76	0.33	0.68	0.77	0.65	0.68	0.76	0.58
4965	0.87	0.91	0.62	0.88	0.91	0.79	0.88	0.91	0.77
4880	1	1	1	1	1	1	1	1	1
4765	1.22	1.15	1.72	1.23	1.14	1.52	1.21	1.14	1.50
4579	1.73	1.47	2.97	1.72	1.44	2.44	1.74	1.45	3.91
4416	2.65	1.90	2.00	2.49	1.84	5.35	2.56	1.86	2.70

Table 4. Theoretically calculated and experimentally observed intensity enhancement for the 1563 cm^{-1} Raman band in terms of the R_A, R_B and R_I factors for TB4A, TB7A and TB10A.

	TB4A			TB7A			TB10A		
λ_o/Å	R_A	R_B	R_I	R_A	R_B	R_I	R_A	R_B	R_I
5145	0.67	0.76	0.35	0.68	0.77	0.65	0.68	0.76	0.58
4965	0.87	0.91	0.59	0.88	0.91	0.79	0.87	0.91	0.73
4880	1	1	1	1	1	1	1	1	1
4765	1.22	1.15	1.86	1.23	1.14	1.52	1.22	1.14	1.58
4579	1.76	1.47	3.47	1.71	1.44	2.44	1.74	1.45	3.49
4416	2.65	1.90	2.38	2.49	1.84	5.40	2.56	1.86	2.68

Table 5. Theoretically calculated and experimentally observed intensity enhancement for the 1195 cm^{-1} Raman band in terms of the R_A, R_B and R_I factors for TB4A, TB7A and TB10A.

	TB4A			TB7A			TB10A		
λ_o/Å	R_A	R_B	R_I	R_A	R_B	R_I	R_A	R_B	R_I
5145	0.67	0.76	0.35	0.69	0.77	0.83	0.68	0.76	0.58
4965	0.87	0.91	0.68	0.88	0.91	0.89	0.88	0.91	0.91
4880	1	1	1	1	1	1	1	1	1
4765	1.22	1.14	1.78	1.23	1.14	1.45	1.21	1.14	1.31
4579	1.77	1.46	2.94	1.72	1.44	2.64	1.74	1.45	2.24
4416	2.64	1.89	2.18	2.48	1.83	3.90	2.55	1.86	1.72

Table 6. Theoretically calculated and experimentally observed intensity enhancement for the 1165 cm^{-1} Raman band in terms of the R_A, R_B and R_I factors for TB4A, TB7A and TB10A.

	TB4A			TB7A			TB10A		
λ_o/Å	R_A	R_B	R_I	R_A	R_B	R_I	R_A	R_B	R_I
5145	0.67	0.76	0.34	0.69	0.77	0.75	0.68	0.77	0.66
4965	0.87	0.91	0.64	0.88	0.92	0.86	0.88	0.91	0.93
4880	1	1	1	1	1	1	1	1	1
4765	1.22	1.14	1.88	1.23	1.14	1.31	1.21	1.14	1.39
4579	1.77	1.46	3.25	1.72	1.44	2.57	1.74	1.45	2.92
4416	2.65	1.89	2.02	2.48	1.83	5.60	2.55	1.85	2.00

shows a peak at the ~457.9 nm excitation line, whereas for TB7A the excitation profile shows the usual monotonic pre-resonance increase. In order to visualize the origin of such an anomaly qualitatively, we subtracted the contribution of the R_A term from the experimentally observed R_I term for each line. The residual enhancement resembles an absorption peak and points towards the possibility of an electronic state having energies in these wavelength regions for TB4A and TB10A, see figures 3(*a*,*c*). However, the absorption spectra of these three compounds do not show any band around the position where the Raman intensity enhancement is anomalous. Therefore, consideration of such an inactive forbidden electronic level as an origin of the above inconsistency may be wrong due to the fact that only dipole-allowed electronic transitions can contribute to the Raman intensity enhancement [15, 19].

Now the outcome of these observations is interesting in two ways. First, TB7A does not show the same REP in comparison with its lower (TB4A) and higher (TB10A) homologues. Second, how would a dipole-forbidden electronic level contribute to the active electronic state so that the observed REPs can be understood satisfactorily? In order to understand the anomaly in intensity enhancement, it is necessary to consider the structures of these compounds. As explained before, the overall structure of the molecules of all three compounds are of the *trans*-type. But for a better understanding we wish now to consider the single crystal X-ray data of the TB$\bar{A}$A homologous series obtained from the studies of Diele *et al.* [26] and the data are reproduced in table 7. A careful examination of these results reveals that for TB7A, the value of the '*a*' lattice parameter is less than that for its lower and higher homologues, and this is a measurable parameter of molecular length in three dimensional lattice co-ordinate systems. For the other members, the '*a*' lattice parameter shows the usual increasing trend due to lengthening of molecules by addition of methylene groups to the terminal chains.

Table 7. Lattice constants of the crystalline phases (after Diele *et al.* [26]).

Compounds	*a*/Å	*b*/Å	*C*/Å	β/degree
TB3A	22.58	5.76	17.59	100.2
TB4A	53.20	5.75	17.57	115.5
TB5A	58.48	5.70	17.94	115.0
TB6A	64.68	5.63	17.39	116.4
TB7A	32.04	5.62	17.59	99.5
TB8A	73.04	5.59	17.59	90.5
TB10A	79.34	5.57	17.39	89.0

This leads to the conclusion that the alkyl chains in TB7A are probably in a *cis*-form, whereas in the TB4A and TB10A molecules the alkyl chains are in the *trans*-form. Again, it is well known that only *trans*-isomers are centro-symmetric [25]. From the above discussion it can therefore be inferred that the TB4A and TB10A molecules are centro-symmetric, whereas TB7A does not possess a centro-symmetric structure.

For centro-symmetric molecules such as all-*trans* linear polyenes [27, 28], diphenyloctatetraene (DPO), and diphenyldecapentaene (DPDP) [29] there exists a lowest singlet excited state known as the 2^1A_g parity forbidden state. The electronic origin of the 2^1A_g state, being of gerade vibronic symmetry, is inaccessible by a one-photon process from the ground state (electronic absorption spectra) due to the alternate parity dipole selection rule [19]. However, such origins have been detected by high resolution fluorescence excitation when the guest molecule is situated in a symmetry-perturbing environment, such as a Shpolskii matrix [30–32].

The present systems TB4A, TB7A and TB10A are spectroscopically less well investigated, and the required data are not available. Therefore the presence of a 2^1A_g parity forbidden level in TB4A and TB10A can only be inferred qualitatively from the fact that the molecules are centro-symmetric in nature. Generally, symmetry-forbidden transitions (2^1A_g as in the present case) have oscillator strengths in the range 10^{-3}–10^{-2} [32] in comparison to $\sim 10^{-6}$ for a singlet–triplet transition. Strong dipole-allowed states, on the other hand, have an oscillator strength of ~1.0–1.5 [27]. Due to the weak oscillator strength, the 2^1A_g parity forbidden level alone could not contribute to the Raman intensity enhancement mechanism [19]. Participation of such weakly allowed states in the intensity enhancement mechanism may be understood by invoking an interference phenomenon between a weakly allowed electronic state and a nearby major active electronic state via vibrational modes [19]. Theoretically such contributions may be understood by considering the Raman scattering intensity, which is proportional to $|\alpha_{\rho\sigma}|^2$, where

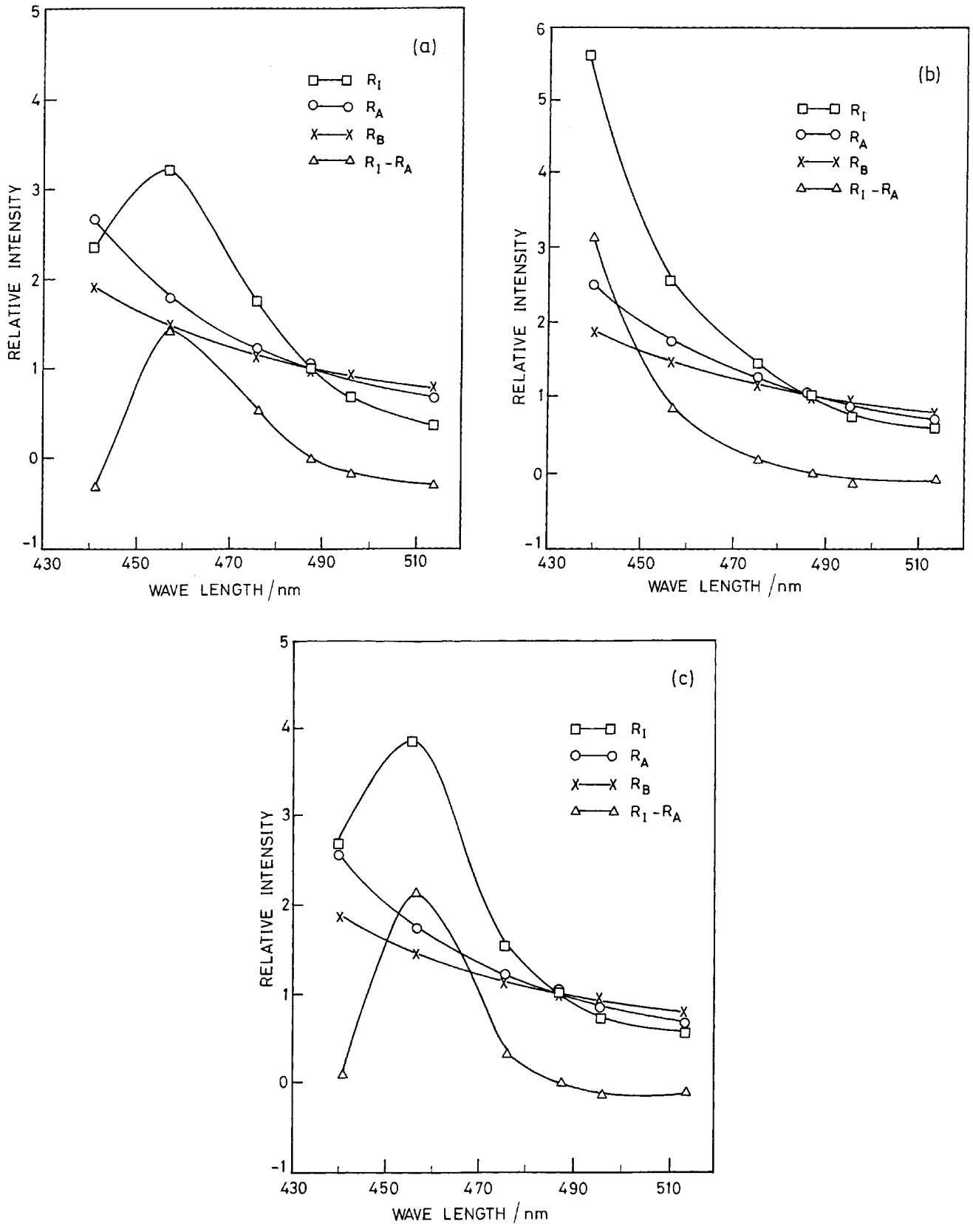

Figure 3. Frequency factors R_A, R_B, R_I with scaling to unity at the 488 nm line and R_I–R_A for the compounds (*a*) TB4A, (*b*) TB7A, (*c*) TB10A.

$\alpha_{\rho\sigma}$ is the polarizability tensor. The polarizability tensor may be expressed by the Kramers–Heisenberg dispersion relation [19, 33]

$$\alpha_{\rho\sigma} = \frac{1}{\hbar}\sum_{l}\left(\frac{\langle F|\mu_\rho|l\rangle\langle l|\mu_\rho|G\rangle}{\omega_l - \omega_0 + i\Gamma_l} + \frac{\langle F|\mu_\sigma|l\rangle\langle l|\mu_\rho|G\rangle}{\omega_l + \omega_0 + i\Gamma_l}\right) \tag{6}$$

where $i\Gamma_l$ is the complex damping factor associated with the vibronic state $|l\rangle$ of energy $\hbar\omega_l$, $\hbar\omega_0$ is the energy of the incident radiation, $\mu_{\rho(\sigma)}$ is the total dipole moment operator (nuclear and electronic) in the $\rho(\sigma)$ direction, and $\langle l|\mu_\sigma|G\rangle$ is the σth component of the transition dipole moment associated with the transition from the initial vibrational level of the ground state $|G\rangle$ to the excited state $|l\rangle$. Similarly, $\langle F|\mu_\rho|l\rangle$ is the ρth component of the transition dipole moment associated with the transition from the $|l\rangle$ excited vibronic state to the final vibrational level of the ground electronic state $|F\rangle$. Moreover, in the near pre-resonance and resonance region of an allowed electronic transition, the first term in equation (6) dominates and we may neglect the contribution from the second term, the anti-resonance term.

We next apply the adiabatic Born–Oppenheimer approximation, whereupon the polarizability tensor $\alpha_{\rho\sigma}$ in equation (6) becomes

$$\alpha_{\rho\sigma} = \frac{1}{\hbar}\sum_{v,m}\frac{\langle u|[\mu_\rho]_{gm}|v\rangle\langle v|[\mu_\sigma]_{mg}|0\rangle}{\omega_v - \omega_0 + i\Gamma_v} \tag{7}$$

where $[\mu_\rho]_{gm} \equiv \langle g|\mu_\rho|m\rangle$ and $[\mu_\sigma]_{mg} \equiv \langle m|\mu_\sigma|_g\rangle$ are components of the pure electronic transition moment, and $|0\rangle$ and $|u\rangle$ are the initial and final ground state vibrational level, respectively. The sum is over all intermediate vibrational levels v of the excited electronic states m. For a totally symmetric vibration of a centro-symmetric linear polyene, only one diagonal element of the polarizability tensor, $\alpha_{\rho\rho}$, need be evaluated [34].

Since the electronic transition moment is a slowly varying function of the internuclear distances, it may be expressed as a rapidly converging power series expanded about the equilibrium position in the normal co-ordinate Q_0 [19]. The first term in the series (known as the A term) will dominate provided that $|(\partial\mu_{gm}/\partial Q)_0| \ll |(\mu_{gm})_0|$. This will be valid for a centro-symmetric linear polyene in the pre-resonance or resonance region for a totally symmetric vibrational mode [35]. In addition, for the case of a dipole-forbidden state, the need for the second term (the B term) in the expansion can be avoided by introducing an empirical value for the forbidden transition moment [19].

Under these conditions, the polarizability expression for such a system with two excited states m and n, reduces to

$$\alpha_{\rho\rho} = \frac{1}{\hbar}\left\{|\mu_{gm}|^2\sum_{v_m}\frac{\langle \bar{u}|\bar{v}_m\rangle\langle \bar{v}_m|\bar{0}\rangle}{\omega_v - \omega_0 + i\Gamma_v} + |\mu_{gn}|^2\sum_{v_n}\frac{\langle \bar{u}|\bar{v}_n\rangle\langle \bar{v}_n|\bar{0}\rangle}{\omega_v - \omega_0 + i\Gamma_v}\right\} \tag{8}$$

where the coefficients $|\mu_{gm}|^2$, $|\mu_{gn}|^2$ are proportional to the corresponding oscillator strengths for the transition from the ground state to the electronic states m and n, respectively. Thus, $f_{mg} = [(4\pi mc)/3\hbar e^2)]\,\nu|\mu_{mg}|^2$, where ν is the wave number of the transition and $|\mu_{mg}|$ is the electronic transition moment [36].

The combination of weakly allowed states to the intensity of the Raman excitation profiles may be understood by considering the Raman scattering intensity which is proportional to $|\alpha_{\rho\sigma}|^2$, where $\alpha_{\rho\sigma}$ is the polarizability tensor. When $\alpha_{\rho\sigma}$ is expressed by the Kramers–Heisenberg dispersion relation of equation (8), it is seen that 'mixing' cross terms arise, which may reduce or enhance the Raman intensity. This is due, in part, to the Frank–Condon integrals, for which the sign is a function of displacement parameter.

As an illustration, let us consider $|\alpha_{\rho\rho}|^2$ obtained from the expression which is given by [37]:

$$|\alpha_{\rho\rho}|^2 = \sum_{i=1}\frac{A_i^2}{\delta\nu^2 + \Gamma_i^2} + \sum_{i=1}\sum_{j=1}\frac{2A_jA_i(\delta\omega_j\delta\omega_i + \Gamma_j\Gamma_i)}{(\delta\omega_j^2 + \Gamma_j^2)(\delta\omega_i^2 + \Gamma_i^2)} \tag{9}$$

where the sum extends over all vibrational states i, ω_i and ω_j are the frequencies of the ith and jth states, $\delta\omega_i = \omega_i - \omega_0$, A_i and A_j are proportional to oscillator strengths and Γ_i and Γ_j are damping factors associated with ith and jth states.

Furthermore, let us consider a system with two electronic excited states, m and n, where the oscillator strength for the state m is much greater than that of state n; $\mu_{gn} \gg \mu_{gm}$. For a given vibrational mode j of the weakly allowed electronic state m, A_j will be very small. Its contribution to the first term of equation (9) may therefore be neglected. The Raman cross terms will then be the only measurable contribution to the Raman intensity, which otherwise may not be detectable within the signal to noise ratio limits of the experiment. However, the proximity of two electronic excited states is a crucial factor in the determination of the intensity level for the interference features in the REP. This can easily be seen from the cross term expression of equation (9). If the incident radiation ω_0 is in resonance with state j then $\delta\omega_j = 0$ and the maximum contribution of the cross terms will occur when the separation between the two coupled electronic excited states is at a minimum, since then $\delta\omega_i$ will also be smallest.

Taking all the above aspects into consideration, it is believed that the electronic origin of the 2^1A_g dipole forbidden electronic state for TB4A and TB10A must lie in the ~ 400 nm region, close to the major electronic state which lies in the ~ 365 nm region in our systems, and the constructive interference between these two electronic states via vibrational modes gives rise to the intensity enhancement at 457 nm region as observed for TB4A and TB10A. Intensity enhancement due to an interference effect has recently been reported by Sztainbuch and Leori [19] in their pre-resonance Raman study on DPDP.

4. Conclusion

We conclude by emphasizing that the three members of the TB$\bar{A}$A homologous series, viz. TB4A, TB7A and TB10A, have a peculiar structural dissimilarity in so far as their vibrational/pre-resonance Raman spectra are concerned. In order to understand the difference in their vibrational Raman spectra in the solid state, the effect of alkyl chain stress on the rigid backbone has been invoked and results in a planar modification of the backbone for molecules having longer alkyl chains. However, due to steric hindrance, the intermolecular backbone spacing is wider for longer molecules than that for smaller molecules. Single crystal X-ray studies show that the long alkyl chains of the molecules have their own adjustable orientation which suits their stability and lower energy configurational state. This is reflected in the fact that TB7A has a smaller molecular length (a probable *cis*-type structure) than that of its lower homologues. This pre-resonance Raman study provides evidence that TB4A and TB10A possess a 2^1A_g dipole-forbidden electronic state originating from their *trans*-type structure.

References

[1] Fontana, M., and Bini, S., 1976, *Phys. Rev. A*., **14,** 1555.
[2] Dvorjetski, D., Volterra, V., and Wiener-Avnear, E., 1975, *Phys. Rev. A*., **12,** 681.
[3] Schnur, J. M., Sheridan, J. P., and Fontana, M., 1975, in Proceedings of the International Liquid Crystal Conference (*Pramana Suppl. no. 1*) edited by S. Chandrasekhar, p. 175.
[4] Schnur, J. M., and Fontana, M., 1974, *J. Phys. (Fr.)*, **35,** L-53.
[5] Bulkin, B. J., Grunbaum, D., Kennelly, T., and Loc, W. B., 1975, in Proceedings of the International Crystal Conference (*Pramana Suppl. no. 1)* edited by S. Chandrasekhar, p. 175.
[6] Schnur, J. M., 1973, *Mol. Cryst. liq. Cryst*., **23,** 155.
[7] Amer, N. M., and Shen, Y. R., 1973, *Solid State Commun*., **12,** 263.
[8] Sakamoto, A., Yosino, K., Kubo, U., and Inuishi, Y., 1974, *Jpn J. appl. Phys*., **13,** 1691.
[9] Dash, S. K., Singh, Ranjan K., Alapati, P. R., and Verma, A. L., 1998, *Mol. Cryst. liq. Cryst*., **319,** 147.
[10] Dash, S. K., Singh, Ranjan K., Alapati, P. R., and Verma, A. L., 1997, *J. Phys.: Condensed Matter*, **9,** 7809.
[11] Albrecht, A. C., and Hutley, M. C., 1971, *J. chem. Phys*., **55,** 4438.
[12] Albrecht, A. C., 1961, *J. chem. Phys*., **34,** 1476.
[13] Lee, S. Y., and Heller, E. J., 1979, *J. chem. Phys*., **71,** 4777.
[14] Page, J. B., and Tonks, D. L., 1981, *J. chem., Phys*., **75,** 5694.
[15] Kiefer, W., 1995, *Infrared and Raman Spectroscopy*, edited by Bernhard Schrader (Weinheim, New York: VCH), Chap. 6, p. 465.
[16] Das Radhendu, and Kumar Kamal, 1989, *Spectrochim. Acta*, **45A,** 705.
[17] Rimai, L., Hyde, M. E., Heller, H. C., and Gill, D., 1971, *Chem. Phys. Lett*., **10,** 207.
[18] Lewis, A., 1973, *J. Raman Spectrosc*., **1,** 473.
[19] Sztainbuch, I. W., Leori, G. E., 1990, *J. chem. Phys*., **93,** 4642.
[20] Gray, G. W., and Goodby, J. W., 1984, *Smectic Liquid Crystals: Textures and Structures* (London: Leonard Hill).
[21] Vergoten, G., and de Jeu, W. H., 1975, *Thermotropic Liquid Crystals: Fundamentals*, Springer series in Liquid Crystals, Vol. 45.
[22] Liebert, L., 1978, *Liq. Cryst. Solid State Phys. Suppl*., **14** (New York: Academic Press).
[23] Alapati, P. R., Potukuchi, D. M., Rao, N. V. S., Pisipati, V. G. K. M., and Saran, D., 1987, *Mol. Cryst. liq. Cryst*., **146,** 111.
[24] Vertogen, G., 1972, *Advances in Raman Spectroscopy*, Vol. 1, edited by J. P. Mathieu (Heyden and Sons), p. 219.
[25] Clothup, N. B., Daly, L. H., and Wiberley, S. E., 1990, *Introduction to Raman and IR Spectroscopy* (Academic Press).
[26] Diele, S., Demus, D., and Sackman, H., 1980, *Mol. Cryst. liq. Cryst*., **56,** 217.
[27] Fang, H. L. B., Thrash, R. J., and Leori, G. E., 1977, *J. chem. Phys*., **67,** 3389.
[28] Fang, H. L. B., Thrash, R. J., and Leori, G. E., 1978, *Chem. Phys. Lett*., **67,** 59.
[29] Hudson, B. S., and Kohler, B. E., 1972, *Chem. Phys. Lett*., **14,** 299.
[30] Simpson, J. H., McLaughlim, L., Smith, D. S., and Christensen, R. L., 1987, *J. chem. Phys*., **87,** 3360.
[31] Hudson, B. S., and Kohler, B. E., 1973, *J. chem. Phys*., **59,** 4984.
[32] Kohler, B. E., Spangler, C., and Westerfield, C., 1988, *J. chem. Phys*., **89,** 5422.
[33] Kramers, H. A., and Heisenberg, W., 1925, *Z. Phys*., **31,** 681.
[34] Mortensen, O. S., and Hassing, S., 1980, *Advances in IR and Raman Spectroscopy*, Vol. 6, edited by R. J. H. Clark and R. E. Hester (London: Heyden), p. 1.
[35] Warshel, A., and Dauber, P., 1977, *J. chem. Phys*., **66,** 5477.
[36] Myers, A. B., and Birge, R. R., 1980, *J. chem. Phys*., **73,** 5314.
[37] Batchelder, D. N., and Bloor, D., 1982, *Advances in IR and Raman Spectroscopy*, Vol. 11, edited by R. T. H. Clark and R. E. Hester (London: Hyden and Sons), p. 133.